Journal of Applied Polymer Science

Synthesis and Characterization of Poly(2,5-didecyl-1,4-phenylene vinylene), Poly(2,5-didecyloxy-1,4-phenylene vinylene), and Their Alternating Copolymer

Crystal A. Young,[1] Sairoong Saowsupa,[1] Audrey Hammack,[2] Andrew A. Tangonan,[1] Piched Anuragudom,[3] Huiping Jia,[2] Andrew C. Jamison,[1] Sukon Panichphant,[4] Bruce E. Gnade,[2] T. Randall Lee[1]

[1]Department of Chemistry and the Texas Center for Superconductivity, University of Houston, Houston, Texas 77204-5003
[2]Departments of Chemistry and Materials Science and Engineering, University of Texas at Dallas, Richardson, Texas 75083
[3]Department of Chemistry, Faculty of Liberal Arts and Science, Kasetsart University, Kamphaeng Saen, Nakhon Pathom 73140, Thailand
[4]Department of Chemistry, Faculty of Science and The Center for Innovation in Chemistry (PERCH-CIC), Chiang Mai University, Chiang Mai 50200, Thailand
Correspondence to: T. R. Lee (E-mail: trlee@uh.edu)

ABSTRACT: The preparation of dialkyl-substituted poly(2,5-didecyl-1,4-phenylene vinylene) (**PDDPV**) by the Horner-Emmons polycondensation is described. Its performance in an organic light-emitting diode (OLED) device architecture is compared with devices prepared from the analogous dialkoxy-substituted poly(2,5-didecyloxy-1,4-phenylene vinylene) (**PDOPV**) and the corresponding alkyl-alkoxy-substituted alternating copolymer. Additionally, the structure, stability, electrochemical, and optical properties of the PPVs were characterized by gel permeation chromatography, thermogravimetric analysis, NMR spectroscopy, cyclic voltammetry, UV-Visible spectroscopy, and fluorescence spectroscopy. © 2014 Wiley Periodicals, Inc. J. Appl. Polym. Sci. **2014**, *131*, 41162.

KEYWORDS: optical and photovoltaic applications; optical properties; polycondensation

Received 16 January 2014; accepted 10 June 2014
DOI: 10.1002/app.41162

INTRODUCTION

Conjugated polymers have been the focus of numerous studies because of their attractive electrical conductivity, nonlinear optical response, and electroluminescent and photoluminescent characteristics.[1–3] Due to these valuable properties, conjugated polymers have been widely investigated for use as active components in electronic and optoelectronic devices (e.g., light-emitting diodes, light-emitting electrochemical cells, photovoltaic cells, field-effect transistors, optocouplers, and optically pumped lasers in solution and in the solid state).[4–9] In particular, the poly(*p*-phenylene vinylene) (PPV) family of conjugated polymers is especially important, owing to their environmental stability and their outstanding photoluminescence and electroluminescence. The addition of selected substituents along the polymer backbone of PPV derivatives can give rise to emissions ranging from green to red light. For example, a soluble PPV with alkoxy side groups, poly[2-methoxy-5-(2-ethylhexyloxy)-1,4-phenylene vinylene] (MEH-PPV), emits at red-shifted wavelengths when compared with simple PPV, which emits light at 580 nm (yellow light).[10] Since 1990, exhaustive studies of the electro-optical properties of PPV and its derivatives have been performed, spurred by the finding that the unmodified neutral state of PPV can be used as a light-emitting layer for organic light-emitting diodes (OLEDs).[11] Currently, a major objective of OLED research centers on the development of light-emitting polymers with both high emission efficiencies and long operation lifetimes, which are intimately related to device performance and reliability.[12,13]

In an OLED, a thin film of light-emitting material is sandwiched between a cathode and an anode, one of which must be semi-transparent to allow the emission of light from the underlying organic layer (see Figure 1). Frequently, glass substrates coated with indium tin oxide (ITO) are used as the anodes, while electropositive metals with low work functions, such as Al, Ca, Mg, or In, are used as the cathodes, providing efficient electron injection.[14] Commercialization of these devices is severely limited by the rapid rate of photo-oxidation of the

Additional Supporting Information may be found in the online version of this article.

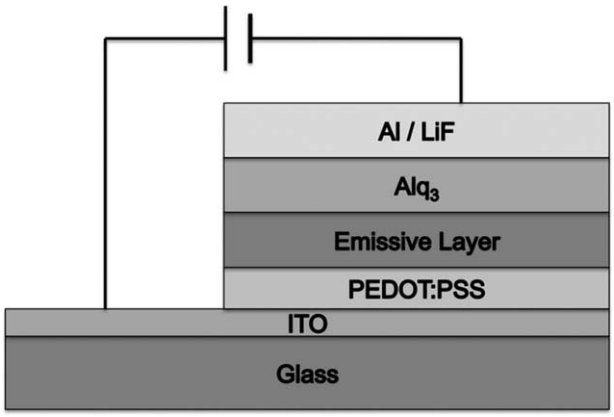

Figure 1. Standard OLED structure.

light-emissive polymer under operational conditions, which deteriorates device performance and ultimately device operation lifetime.[13] Working devices, such as flat-panel displays employing blue OLEDs have been plagued by limited lifetimes in the range of 1,000 h at constant voltage, which is markedly lower than the typical lifetimes of LCD- or plasma-based flat-panel displays.[15]

Another concern is related to their extended conjugation length and enhanced electron delocalization; conjugated polymers in OLED devices are highly susceptible to photooxidation by singlet oxygen during device operation.[16,17] Furthermore, the presence of electron-donating alkoxy groups on the phenyl rings lowers the oxidation potential of the polymers (vide infra), which plausibly further enhances the oxidative degradation of their relatively fragile conjugated backbones. Specifically, Cumpston and Jensen proposed that the presence of alkoxy groups promotes the 1,2-cycloaddition of singlet oxygen to the vinyl bonds of the polymer backbone, leading to the oxidative cleavage of the polymer chain as shown, for example, in Figure 2.[16–18]

Overwhelming evidence suggests that both the degradation of the electroluminescent polymer and oxidation of the electrodes are culprits of device failure.[14,15] Strategies to frustrate these processes to improve device operation lifetime and performance are generally centered either on the modification of the electrodes or the transport layer. Consequently, recent studies have focused on varying the composition of selected OLED layers to improve the active lifetime; specific examples include doping the hole-transport or hole-injection layer of the device,[19,20] which markedly enhances performance, but fails to address the issue of photooxidation of the light-emitting material. As shown in Figure 2, the photooxidation of PPVs gives rise to polar functional groups, such as carbonyls, acids, esters, and alcohols, along with chain scissions and crosslinks that compromise the inherent properties of the polymers, including their dielectric properties and transparency. Consequently, alternative strategies have sought to block the photodegradation process via inhibition with chain-breaking acceptors, chain-breaking donors, UV absorbers, metal deactivators, stoichiometric decomposers, catalytic peroxide decomposers, and excited-stated quenchers.[21]

In addition to addressing issues related to component stability and increasing overall device operation lifetime, research has also focused on the development of new polymers to control the color of the emitted light and improve the efficiency of emission. While a wide variety of poly(arylene vinylene)s have been synthesized and used in OLED device architectures, three synthetic approaches—Gilch polymerization, Wessling precursor elimination, and Wittig polycondensation—are predominantly used for their preparation.[22–24] Two major concerns associated with the former, and increasingly popular route, are the formation of (1) insoluble gels and (2) polymers with saturated defects. In contrast, we have found that an appropriately designed Horner-Emmons coupling affords defect-free conjugated polymers with respectable molecular weight characteristics.[25,26]

While the majority of synthetic efforts have targeted soluble PPVs with alkoxy substituents attached to the phenyl rings, which are ubiquitous in polymer-based OLED devices, our research seeks to prepare soluble PPVs with alkyl groups attached to the aromatic rings. As noted above, the absence of strongly electron-donating alkoxy groups is likely to reduce the rate of oxidative degradation and thus enhance device performance and operation lifetime.[14] Moreover, the introduction of

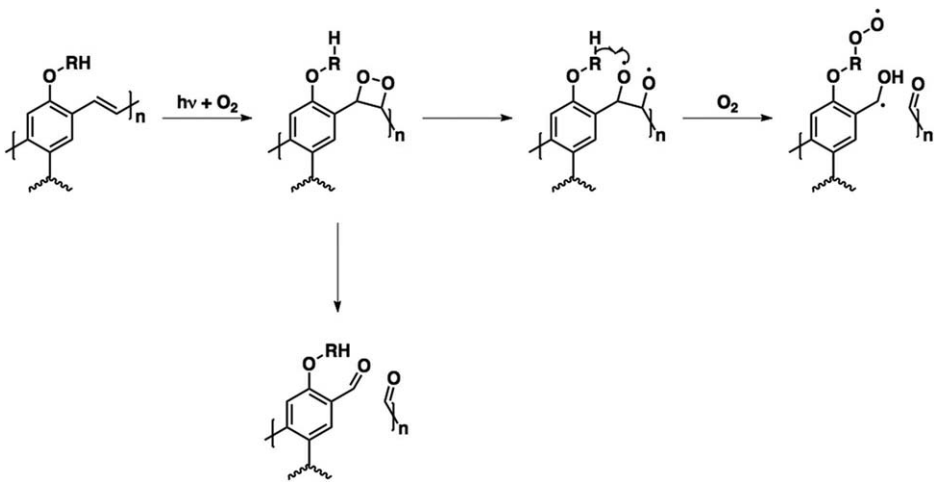

Figure 2. Proposed mechanism for the oxidation of alkoxy-substituted PPVs.[16,17]

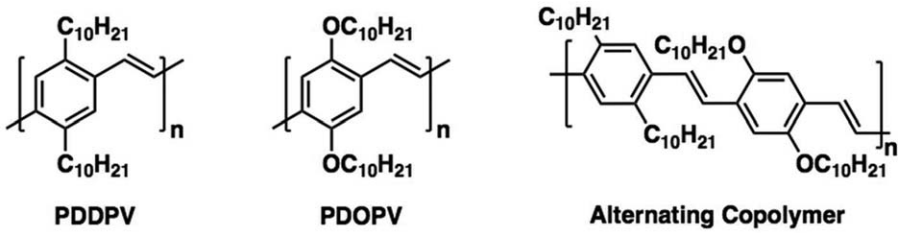

Figure 3. Chemical structures of the three conjugated polymers.

two additional oxidizable benzylic hydrocarbon moieties per aromatic ring is expected to provide additional improvement to device performance and operation lifetime. In particular, these additional oxidizable positions can serve as sacrificial oxidant scavengers without loss of conjugation.

To this end, we report here the preparation of dialkyl-substituted poly(2,5-didecyl-1,4-phenylene vinylene) (**PDDPV**) and compare its structure, optical properties, electrochemical properties, and performance in a device architecture to the analogous dialkoxy-substituted poly(2,5-didecyloxy-1,4-phenylene vinylene) (**PDOPV**) and the corresponding alkyl-alkoxy-substituted alternating copolymer (**PDDPV-alt-DOPV**) (see Figure 3).

EXPERIMENTAL

Instrumentation

^{1}H NMR spectra were recorded using either a JEOL ECA-500 or a JEOL ECX-400P spectrometer. The data were processed using Delta NMR data processing software. The corresponding spectra are provided in Figures S1 to S14 of the Supporting Information. Chemical shifts are reported in δ (ppm) relative to internal standards chloroform-d_1 ($CDCl_3$) and tetrahydrofuran-d_8 (THF-d_8), purchased from Cambridge Isotope Laboratories. Chemical shifts for ^{1}H NMR were referenced to δ 7.26 for $CDCl_3$ or to δ 3.58 for THF-d_8. ^{13}C NMR spectra were recorded using a General Electric QE-300 spectrometer (300 MHz) and the data processed using NUTSNMR Utility Transform Software (Acorn NMR). Molecular weights and polydispersities were determined by gel permeation chromatography (GPC) in THF relative to polystyrene standards, giving the number-average molecular weights (M_n) and the weight-average molecular weights (M_w) of the polymers. The samples were injected at a flow rate of 1 mL/min through a series of two Waters Styragel HR 5E (7.8 $\times$ 300 nm) columns equipped with a Waters 410 differential refractometer and Waters 996 photodiode array detector. No effort was made to correct the molecular weights for differences in the Mark-Houwink coefficient and exponent. The data were analyzed using Waters Millennium 2010 Chromatography Manager GPC software (version 2.0). UV-Vis spectrophotometry with baseline corrections and normalizations was performed using an 8453 Agilent UV-visible system. Fluorescence spectra were recorded in THF using a Perkin Elmer LS 45 Luminescence spectrometer. Thermal gravimetric analysis of polymers and copolymers were measured on a TA Instruments 2050 thermogravimetric analyzer (TGA) instrument with a heating rate of 10°C min^{-1}. Cyclic voltammetric (CV) measurements were performed in acetronitrile (CH_3CN) with 0.1*M* tetrabutylammonium hexafluorophosphate ($TBAPF_6$) as the supporting electrolyte at a scan rate of 100 mV/s. Platinum wires were used as the counter electrode, silver/silver ions (Ag in 0.1*M* $AgNO_3$ solution, from Bioanalytical Systems, Inc.) were used as the reference electrode. The measurement was performed under a slow bubbling of nitrogen gas at room temperature.

MATERIALS

1,4-Dichlorobenzene (**1**), 1,3-bis(diphenylphosphino)propane nickel(II) chloride [$NiCl_2$(dppp)], 1-bromodecane, bromine, copper cyanide (CuCN), potassium *tert*-butoxide (1.0*M* solution in THF), diisobutylaluminium hydride (DIBAL-H in toluene), paraformaldehyde, 33% hydrobromic acid in HOAc, triethylphosphite, 9,10-diphenylanthracene, quinine sulfate, 1,2-dichlorobenzene (ODCB), and hydroquinone were purchased from either Acros or Aldrich Chemical Co. and used without further purification, unless otherwise noted. In synthetic preparations, diethyl ether and tetrahydrofuran (THF) were acquired from Aldrich Chemical Co. and dried by distillation from CaH_2 under nitrogen. Anhydrous dimethyl sulfoxide and anhydrous dimethylformamide (DMF) were purchased from Aldrich Chemical Co. and used as received. Column chromatography was performed using silica gel (Merck, 250–430 mesh). Fused quartz microscope slides were purchased from AdValue Technology. For the preparation of the devices, Clevios^{TM} PEDOT : PSS was purchased from Heraeus Precious Metals. Tris(8-hydroxyquinolinato)-aluminum (Alq3; sublimed) was acquired from Luminescence Technology Corp. and lithium fluoride (LiF; anhydrous) was purchased from Sigma-Aldrich, while the 1.0 mm diameter aluminum wire (99.999%) was purchased from Kurt J. Lesker Co.

Device Fabrication and Measurements

The devices were fabricated on indium tin oxide (ITO) patterned glass with a sheet resistance of 15 Ω/sq. After solvent cleaning, the substrates were treated with reactive ion etching (RIE). PEDOT : PSS filtered through a 0.45 μm syringe filter was spin-coated at 2000 rpm for 1 min and baked at 120°C for 1 h to remove water. Polymer solutions (10 mg/mL in ODCB) were stirred overnight at 40°C and for 1 h prior to spin coat application at 100°C. The solutions were filtered through 0.45 μm syringe filters, spin-coated on the device surface at 700 RPM for 90 s, and baked at 70°C overnight before cathode deposition. Thin films of Alq3, LiF, and Al were deposited using a thermal evaporator (Cooke Vacuum Systems Inc.) at a base pressure of 2.0 $\times$ 10^{-6} torr. The devices were tested without encapsulation using a Keithley 236 source meter, working with a customized version of SpectraWin 2 software and a PR-650 SpectraScan spectrophotometer.

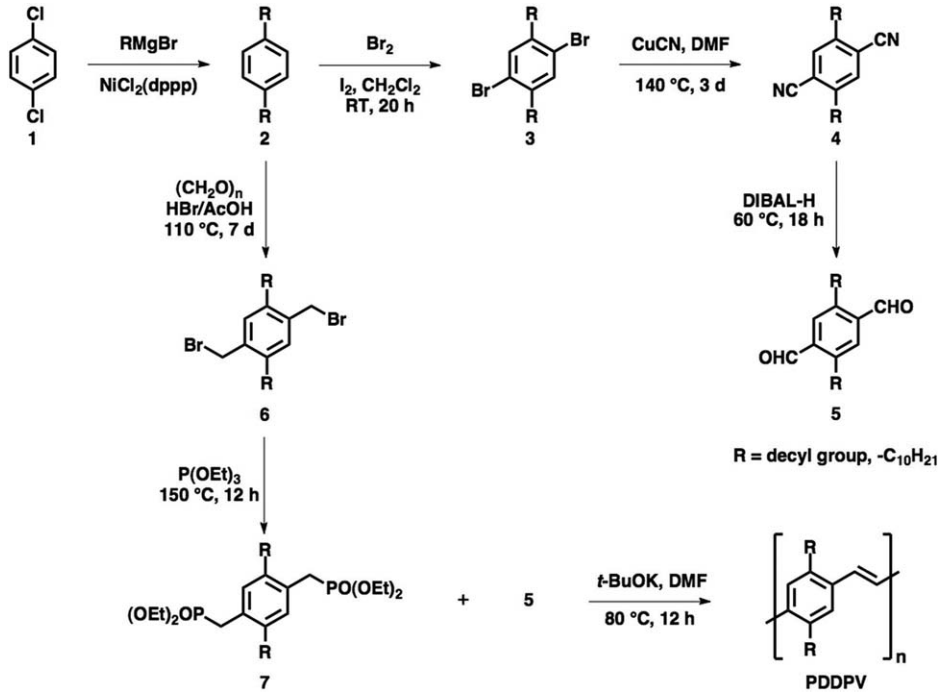

Scheme 1. Strategy Used to Prepare Polymer PDDPV. [Color figure can be viewed in the online issue, which is available at wileyonlinelibrary.com.]

Synthesis of Monomers and Polymers

Scheme 1 illustrates the strategy used to prepare dialkyl-substituted poly(2,5-didecyl-1,4-phenylene vinylene) (**PDDPV**).

1,4-Didecylbenzene (2). In a 1000 mL three-neck flask, 20.18 g (0.8301 mol) of magnesium turnings and 200 mL of dry diethyl ether were combined. An addition funnel containing 100 mL (0.479 mol) of 1-bromodecane was attached, and approximately 5 mL was added to initiate the reaction. The solution was kept at a low boil while the rest of the 1-bromodecane was added dropwise over 1 h. Afterwards, the mixture was refluxed at 45°C for 45 min and then cooled to 0°C. A solution of 44.1 g (0.300 mol) 1,4-dichlorobenzene **1** and 0.57 g (1.1 mmol) of [$NiCl_2$(dppp)] in 200 mL dry diethyl ether was transferred by cannula into the freshly prepared Grignard solution. The brownish colored mixture was stirred vigorously until the diethyl ether started to boil. To aid stirring, an additional 300 mL of dry diethyl ether was added and the suspension was then refluxed for 6 h and stirred overnight at room temperature. The cooled mixture (0°C) was carefully quenched with 600 mL 2*M* HCl and the aqueous fraction was extracted with diethyl ether. The combined ether layers were washed with water, sodium bicarbonate solution, and brine, and then dried over Na_2SO_4. After evaporating the solvent, the product was obtained by vacuum distillation at 180°C to give a light yellow crystalline solid (86.07 g, 80%). ^{1}H NMR (400 MHz, $CDCl_3$): δ 0.87 (t, $J = 6.4$ Hz, 6H, CH_3), 1.20–1.35 (m, 28H, CH_2), 1.55–1.62 (m, 4H, β-CH_2), 2.55 (t, $J = 7.8$ Hz, 4H, α-CH_2), 7.08 (s, 4H, aromatic).

1,4-Dibromo-2,5-didecylbenzene (3). To a chilled solution (10°C) of 0.14 g (0.55 mmol) iodine in 15.0 g (41.8 mmol) of **2**, 30.0 g (188 mmol) bromine dissolved in 30 mL CH_2Cl_2, were added dropwise within 2 h and under rigorous exclusion of light. After 20 h at room temperature, 20% KOH solution was added carefully until the red color disappeared. The aqueous layer was decanted and the organic layer was washed with water and brine, and then dried over Na_2SO_4. After evaporating the solvent, a light yellow solid **3** was obtained, which was recrystallized in ethanol (19.20 g, 89%). ^{1}H NMR (400 MHz, $CDCl_3$): δ 0.87 (t, $J = 6.9$ Hz, 6H, CH_3), 1.22–1.39 (m, 28H, CH_2), 1.51–1.60 (m, 4H, β-CH_2), 2.62 (t, $J = 8.3$ Hz, 4H, α-CH_2), 7.34 (s, 2H, aromatic).

2,5-Didecylterephthalonitrile (4). Under argon, 12.00 g (23.24 mmol) of 1,4-dibromo-2,5-didecylbenzene **3** and 7.00 g (78.2 mmol) of fresh CuCN were placed in a 250 mL round bottom flask. After the addition of 150 mL of dry DMF, the suspension was refluxed for 3 days. The solution was cooled to room temperature and poured into a flask containing 300 mL of 25% aq. NH_3 to precipitate the product. The product was washed with 25 mL of 25% aq. NH_3 and 200 mL of water. The remaining material was extracted in a Soxhlet apparatus with acetone (300 mL) for 12 h. The solvent was evaporated to yield a light yellow solid (6.84 g, 72%). ^{1}H NMR (400 MHz, $CDCl_3$): δ 0.87 (t, $J = 6.8$ Hz, 6H, CH_3), 1.21–1.40 (m, 28H, CH_2), 1.61–1.69 (m, 4H, β-CH_2), 2.81 (t, $J = 7.8$ Hz, 4H, α-CH_2), 7.53 (s, 2H, aromatic).

2,5-Didecylterephthalaldehyde (5). Under argon, to a solution of 4.10 g (10.0 mmol) 2,5-didecylterephthalonitrile **4** in 25 mL toluene, 25 mL (38 mmol) of a 1.5*M* solution of DIBAL-H in toluene was added dropwise for a period of 60 min. After warming the solution to 65°C, the mixture was stirred for 18 h, cooled to 0°C and hydrolyzed with 100 mL of a MeOH/water solution (40 : 60). The suspension was poured into 150 mL of

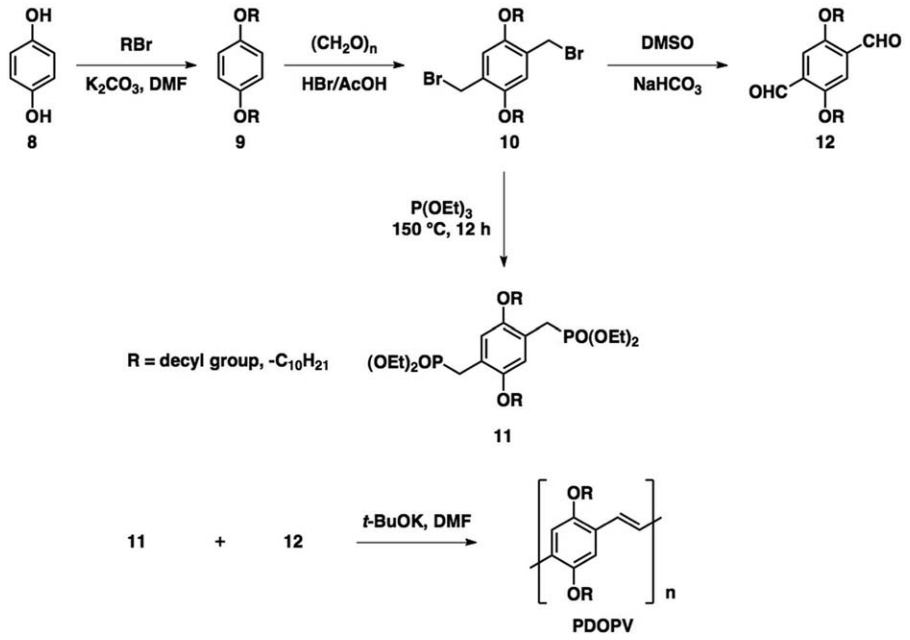

Scheme 2. Strategy Used to Prepare Polymer PDOPV.

2*M* HCl and stirred for 1 h to dissolve the aluminum salts. The aqueous layer was extracted with diethyl ether and the resulting organic layer was dried over Na_2SO_4. The solvent was evaporated to give the product as a yellow powder. The crude product was filtered through silica gel (petroleum ether : chloroform, 1 : 2, as the eluent). Compound **5** was obtained as a light yellow powder (2.04 g, 49%). ^{1}H NMR (500 MHz, $CDCl_3$): δ 0.87 (t, $J = 6.9$ Hz, 6H, CH_3), 1.21–1.34 (m, 24H, CH_2), 1.34–1.41 (m, 4H, CH_2), 1.58–1.64 (m, 4H, β-CH_2), 3.02 (t, $J = 8.1$ Hz, 4H, α-CH_2), 7.71 (s, 2H, aromatic), 10.35 (s, 2H, –CHO).

1,4-Bis(bromomethyl)−2,5-didecylbenzene (6). A 100 mL cylindrical high pressure glass vessel equipped with a magnetic stirring bar was charged with 4.00 g (11.2 mmol) of **2**, 24 mL of acetic acid, 1.22 g (40.5 mmol) of paraformaldehyde, and 4.84 mL of 33 wt % hydrobromic acid in acetic acid. The resulting mixture was heated with stirring at 110°C for 7 days. Additional hydrobromic acid solution and paraformaldehyde were added twice during the course of the reaction. 30 mL of water was added to precipitate the product. After filtering, the white solid was dissolved by heating in diethyl ether and hexanes (4 : 1) and was transferred to a separatory funnel. After washing with water, saturated $NaHCO_3$ solution and brine, the resulting organic layer was dried over magnesium sulfate. The solvent was removed under vacuum, and a yellow solid was obtained. The product was recrystallized twice in hexanes to give the yellow powder of **6** (3.40 g, 56%). ^{1}H NMR (400 MHz, $CDCl_3$): δ 0.86 (t, $J = 6.8$ Hz, 6H, CH_3), 1.21–1.39 (m, 24H, CH_2), 1.40–1.51 (m, 4H, CH_2), 1.75–1.82 (m, 4H, β-CH_2), 3.98 (t, $J = 6.4$ Hz, 4H, α-CH_2), 4.51 (s, 4H, CH_2Br), 6.83 (s, 2H, aromatic).

1,4-Bis(diethylphosphonate)−2,5-didecylbenzene (7). A mixture of **6** (3.00 g, 5.51 mmol) and triethylphosphite (4.60 g, 27.7 mmol) was stirred at 160 °C for 12 h. The unreacted triethyl phosphite was removed by vacuum distillation at 175 to 180°C. A total of 3.60 g of white solid was obtained (yield: 99%). ^{1}H NMR (500 MHz, $CDCl_3$): δ 0.85 (t, $J = 6.9$ Hz, 6H, CH_3), 1.20 (t, $J = 6.9$ Hz, 12H, -OCH_2CH_3), 1.20–1.37 (m, 28H, CH_2), 1.48–1.55 (m, 4H, β-CH_2), 2.59 (t, $J = 8.0$ Hz, 4H, α-CH_2), 3.11 (d, 4H, $J = 20.1$, CH_2P), 3.89–4.10 (m, 8H, -OCH_2CH_3), 7.07 (d, $J = 1.2$ Hz, 2H, aromatic).

Poly(2,5-didecyl-p-phenylene vinylene) (PDDPV). The didecylterephthalaldehyde **5** (0.99 g, 2.4 mmol) and monomer **7** were dissolved in 50 mL of anhydrous DMF under argon. To this solution, potassium *tert*-butoxide (1.34 g, 11.9 mmol) was added. The reaction mixture was stirred overnight at 80°C under nitrogen. The polymer was precipitated from 200 mL of methanol, and the resulting suspension was centrifuged. The supernatant was decanted, and the polymer residue was redissolved in a minimum amount of THF. The crude polymer was then successively reprecipitated from methanol, 2-propanol, and pentane to remove oligomers and small-molecule impurities. The final product was dried under vacuum to afford the polymer **PDDPV** as a bright yellow-green solid (0.59 g, 65%). ^{1}H NMR (500 MHz, $CDCl_3$): δ 0.82–0.87 (m, 6H, CH_3), 1.20–1.48 (m, 28H, CH_2), 1.62–1.72 (m, 4H, β-CH_2), 2.74–2.80 (m, 4H, α-CH_2), 7.23 (peak obscured by residual $CHCl_3$), 7.41 (2H, aromatic). ^{1}H NMR (500 MHz, THF-d_8): δ 0.82–0.88 (m, 6H, CH_3), 1.18–1.48 (m, 28H, CH_2), 1.62–1.72 (peak obscured by residual THF), 2.74–2.84 (m, 4H, α-CH_2), 7.28 (s, 2H, vinylene), 7.44 (2H, aromatic). ^{13}C NMR (75 MHz, $CDCl_3$): d 14.1, 23.2, 26.7, 26.8, 29.9, 30.1, 30.2, 30.3, 32.4, 122.5, 126.0, 128.8, 140.6.

Scheme 2 illustrates the strategy used to prepare the dialkoxy-substituted poly(2,5-didecyloxy-1,4-phenylene vinylene) (**PDOPV**).

1,4-Bis(decyloxy)benzene (9). A white solid **9** was obtained (32.43 g, 83% yield).[27] ^{1}H NMR (400 MHz, $CDCl_3$): δ 0.87 (t, $J = 6.9$ Hz, 6H, CH_3), 1.21–1.38 (m, 24H, $OCH_2CH_2CH_2(CH_2)_6CH_3$), 1.39–1.46 (m, 4H, $OCH_2CH_2CH_2R$), 1.74 (quintet, $J = 6.9$ Hz, 4H,

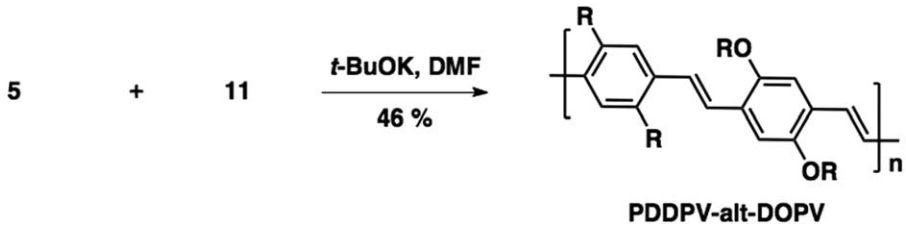

Scheme 3. Strategy Used to Prepare Copolymer PDDPV-alt-DOPV.

OCH_2CH_2R'), 3.88 (t, $J = 6.9$ Hz, 4H, OCH_2R''), 6.81 (s, 4H, aromatic).

2,5-Bis(bromomethyl)-1,4-bis(decyloxy)benzene (10). To a suspension of **9** (14.80 g, 37.88 mmol) and paraformaldehyde (5.68 g, 189 mmol) in acetic acid (125 mL) was added HBr (16 mL, 33 wt % in acetic acid) all at once. The mixture was then added to a pressure vessel and heated at 60 to 70°C for 5 h. After cooling to room temperature, this suspension was poured into water. The precipitate that formed was filtered and then dissolved in hot chloroform. The resulting solution was reprecipitated from methanol to give **10** (19.0 g, 87%) as a white solid after filtration, which was then dried under vacuum. ^{1}H NMR (400 MHz, $CDCl_3$): δ 0.86 (t, $J = 6.8$ Hz, 6H, CH_3), 1.21–1.38 (m, 24H, $-OCH_2CH_2CH_2(CH_2)_6CH_3$), 1.43–1.51 (m, 4H, $OCH_2CH_2CH_2R$), 1.79 (quintet, $J = 6.4$ Hz, 4H, OCH_2CH_2R'), 3.93 (t, $J = 4.6$ Hz, 4H, OCH_2R''), 4.51 (s, 4H, CH_2Br), 6.84 (s, 2H, aromatic).

1,4-Bis(diethylphosphonate)-2,5-didecyloxybenzene (11). A mixture of **10** (6.50 g, 11.3 mmol) and triethylphosphite (11.20 g, 67.41 mmol) was stirred at 150°C for 12 h. The remaining triethyl phosphite was removed by vacuum distillation. A white solid was obtained which was dried under vacuum (7.40 g, 95%). ^{1}H NMR (500 MHz, $CDCl_3$): δ 0.87 (t, $J = 7.4$ Hz, 6H, CH_3), 1.22 (t, $J = 7.5$ Hz, 12H $-OCH_2CH_3$), 1.25–1.35 (m, 28H, CH_2), 1.39–1.45 (m, 4H, CH_2), 1.75 (quintet, $J = 8.1$ Hz, 4H, CH_2), 3.21 (d, $J = 20.1$ Hz, 4H, CH_2P), 3.90 (triplet, $J = 6.9$ Hz, 4H, CH_2), 4.01 (dquint, $J = 7.2$ Hz, 1.7 Hz, 8H), 6.90 (d, $J = 1.7$ Hz, 2H, aromatic). 3.89–4.10 (m, 8H, $-OCH_2CH_3$), 7.07 (d, $J = 1.2$ Hz, 2H, aromatic).

2,5-Bis(decyloxy)benzene-1,4-dialdehyde (12). The final product was a yellow solid (1.33 g, 59%).[28] ^{1}H NMR (400 MHz, $CDCl_3$): δ 0.87 (t, $J = 6.8$ Hz, 6H, CH_3), 1.21–1.39 (m, 24H, $OCH_2CH_2CH_2(CH_2)_6CH_3$), 1.42–1.49 (m, 4H, $OCH_2CH_2CH_2R$), 1.82 (quintet, $J = 7.8$ Hz, 4H, OCH_2CH_2R'), 4.07 (t, $J = 6.4$ Hz, 4H, OCH_2R''), 7.42 (s, 2H, aromatic), 10.51 (s, 2H, CHO).

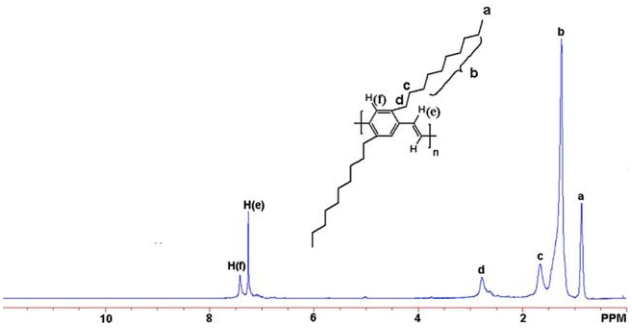

Figure 4. 300 MHz ^{1}H-NMR spectrum of poly(2,5-didecyl-1,4-phenylene vinylene) (**PDDPV**). [Color figure can be viewed in the online issue, which is available at wileyonlinelibrary.com.]

Poly(2,5-didecyloxy-p-phenylene vinylene) (PDOPV). PDOPV was prepared following a procedure similar to that of **PDDPV**.[29] The dialdehyde **12** (0.0684 g, 0.153 mmol) and monomer **11** (0.1003 g, 0.1452 mmol) were dissolved in 40 mL of anhydrous DMF that was degassed under nitrogen. To this solution, potassium *tert*-butoxide (0.86 g, 0.76 mmol) was added. The reaction mixture was stirred for 24 h at 100°C under argon. The polymer was precipitated from 200 mL of methanol, and the resulting suspension was centrifuged. The supernatant was decanted, and the polymeric residue was redissolved in a minimum amount of THF. The crude polymer was then successively reprecipitated from methanol twice, isopropanol, and hexanes, to remove oligomers and small-molecule impurities. The final product was dried under vacuum to afford the polymer **PDOPV** as a red solid (0.054 g, 84%). ^{1}H NMR (400 MHz, $CDCl_3$): δ 0.84–0.88 (m, 6H, CH_3), 1.25–1.53 (m, 24H, CH_2), 1.45–1.66 (m, 4H, CH_2), 1.77–1.91 (m, 4H, β-CH_2), 3.95–4.09 (m, 4H, α-CH_2), 7.15 (d, $J = 12$ Hz, 2H, *trans*-vinylene), 7.45 (s, 2H, aromatic). ^{13}C NMR (75 MHz, $CDCl_3$): δ 14.1, 23.2, 26.7, 26.8, 29.9, 30.1, 30.2, 30.3, 32.4, 122.5, 126.0, 128.8, 140.6.

Alternating Copolymer, Poly(2,5-didecyl-p-phenylene vinylene-alt-2,5-didecyloxy-p-phenylene vinylene) (PDDPV-*alt*-DOPV). This polymer was prepared as illustrated in Scheme 3. To a stirred solution of didecylterephthalaldehyde **5** (0.15 g, 0.36 mmol) and monomer **11** (0.24 g, 0.36 mmol) in 20 mL of DMF at 80°C under nitrogen was added 0.20 g (1.8 mmol) of *t*-BuOK. The reaction mixture was stirred overnight. The resulting orange product was precipitated from 100 mL of methanol and the suspension was centrifuged. The supernatant was decanted and the residue was redissolved in a minimum amount of THF. The crude polymer was reprecipitated successively from methanol, 2-propanol, and pentane. The final product was dried under vacuum to afford an orange solid (0.13 g, 46 %). ^{1}H NMR (500 MHz, $CDCl_3$): δ 0.83–0.89 (m, 12H, CH_3), 1.17–1.52 (m, 52H, CH_2), 1.55 (m, 4H, β-CH_2), 1.61–1.71 (m, 4H, β-CH_2) 1.84–1.91 (m, 4H, β'-CH_2), 2.71–2.79 (m, 4H, α-CH_2), 4.08 (m, 4H, α'-CH_2), 7.12 (s, 2H, aromatic), 7.36 (d, $J = 12.0$ Hz, 2H, *trans*-vinylene), 7.44 (s, 2H, aromatic). ^{13}C NMR (75 MHz, $CDCl_3$): d 14.1, 22.7, 26.2, 26.3, 29.34, 29.6, 29.6, 29.67, 30.3, 31.4, 31.9, 69.6, 96.0, 122.5, 125.45, 126.7, 151.1.

RESULTS AND DISCUSSION

Monomer and Polymer Synthesis

Two PPV homopolymers along with an alternating copolymer were synthesized to act as the light–emitting chromophores in the active layer of an OLED. The chemical structures of the

Table I. Summary of Reaction Yields, Molecular Weights, and Optical Properties

Polymer	Yield (%)	M_W[a] (g mol^{-1})	M_n[a] (g mol^{-1})	PDI[b]	UV-Vis λ_{max} (nm)	FL λ_{max} (nm)	QY[e] (%)
PDDPV	65	8,700	5,200	1.7	380[c], 385[d]	496[c], 507[d]	57
PDOPV	84	5,700	3,500	1.6	465[c], 485[d]	535[c], 582[d]	34
PDDPV-alt-DOPV	46	19,700	8,800	2.2	440[c], 470[d]	510[c], 543[d]	44

[a] M_w = weight-average mol. wt.; M_n =number-average mol. wt.
[b] Polydispersity index (PDI) = M_w/M_n.
[c] Absorption (UV-Vis) and fluorescence (FL) maxima on $1.5 \times 10^{-5}M$ solutions in THF.
[d] Absorption (UV-Vis) and fluorescence (FL) maxima on $1.5 \times 10^{-5}M$ solutions on quartz slides spin coated from 5 mg/mL solutions in *O*-DCB.
[e] Photoluminescent quantum yield in THF relative to 9,10-diphenylanthracene and quinine sulfate. Alternate molecular weight data for samples used in TGA and CV measurements can be seen in the Supporting Information.

homopolymers and the associated alternating copolymer are depicted in Figure 3. The substitution pattern (decyl/decyloxy side chains) in the homopolymers and the alternating copolymer were varied in order to tune the wavelength of light emission with a goal of creating an emission in the blue to orange/red wavelength region. Additionally, the substitution of the decyl side chains in place of the decyloxy side chains provides an opportunity to determine if the change in structure at the benzylic position of the side chains affects the resistance to oxidation for these conjugated polymer systems.

Synthesis of Poly(2,5-didecyl-1,4-phenylene vinylene) (PDDPV). The synthetic procedure utilized to successfully prepare our polymers is based upon recent research by Lee and co-workers demonstrating the benefits of the Horner-Emmons route to prepare soluble light-emitting aryl-vinylene conjugated polymers.[25,26] The Horner-Emmons polycondensation reaction of dialdehydes with bisphosphonate esters is convenient and inexpensive. Although reports that the ADMET polymerization procedure appears to afford the desired materials, this method requires air-free conditions and an expensive transition metal-based polymerization initiator.[30] And while the Gilch route can generate polymers with a higher molecular weight and sometimes with lower polydispersities than the polymers generated by the Horner-Emmons route, the Gilch method is not as consistent in producing defect-free structures; for example, occurrences of saturation along the polymer backbone are common.[22–25]

Our attempt at obtaining the optimum conditions for preparing these polymers can be seen with the Horner-Emmons route shown in Scheme 1. While this procedure assists in the production of a consistent polymer, specific steps were taken to ensure an adequate product yield possessing both a high molecular weight and a low polydispersity. The reaction mixture was treated with an excess of potassium *tert*-butoxide under controlled conditions, which was then stirred for 24 h. Additionally, the product was purified by a series of reprecipitations, working with several solvents, as described in the Experimental Section, with product isolation by centrifuge.

The ^{1}H-NMR spectra of the final polymerized product, **PDDPV**, shows two broad signals in the aromatic region at 7.41 ppm and 7.23 ppm corresponding to aromatic protons and *trans*-vinylene protons in a conjugated system, respectively, as shown in Figure 4. There is no sign of dialdehyde proton resonances at around 10.50 ppm, which would be characteristic for one of the monomers, indicating its absence. The product peak at 2.77 ppm is from the chemical shift of the α-methylene protons. Importantly, no saturated defects are observed at ~3.1 ppm.[23–25]

Synthesis of Poly(2,5-didecyloxy-1,4-phenylene vinylene) (PDOPV). Scheme 2 shows the synthetic route used to prepare ***PDOPV.***

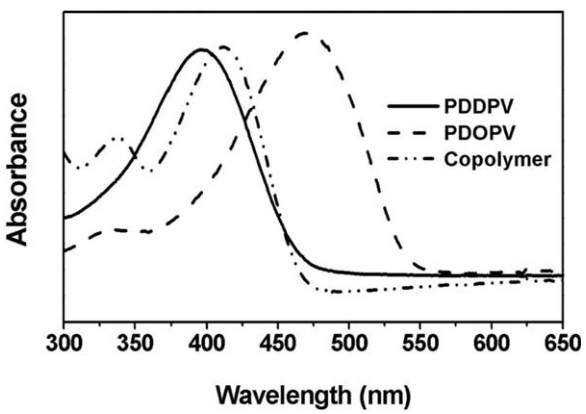

Figure 5. Absorption spectra of **PDDPV**, **PDOPV**, and **PDDPV-alt-DOPV** prepared by Horner-Emmons polymerization. Samples were dissolved in THF ($1.5 \times 10^{-5}M$) and recorded at room temperature.

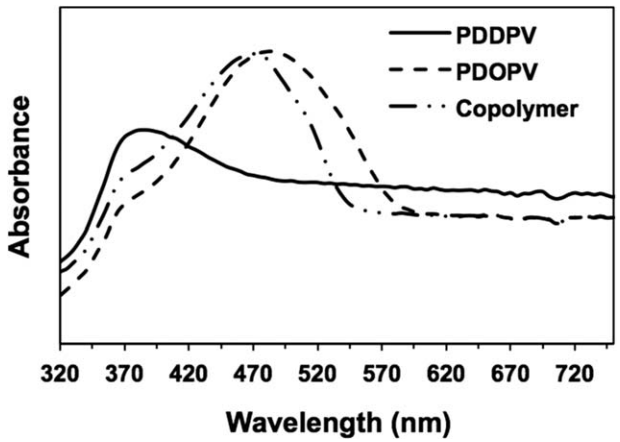

Figure 6. Film absorption spectra of **PDDPV**, **PDOPV**, and **PDDPV-alt-DOPV** prepared by Horner-Emmons polymerization. Samples were dissolved in ODCB (1 mg/mL) and spin coated on quartz slides.

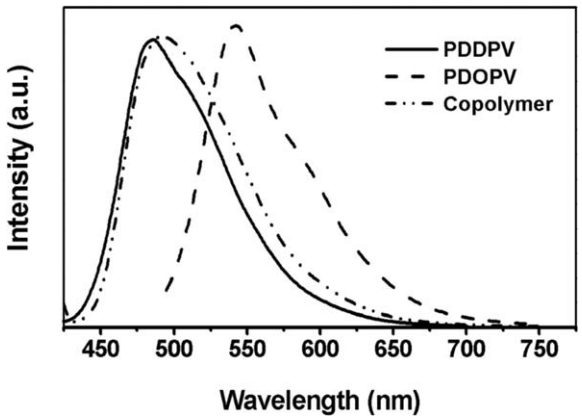

Figure 7. Fluorescence spectra of **PDDPV** (excitation at 380 nm), **PDOPV** (excitation at 465 nm), and **PDDPV-alt-DOPV** (excitation at 440 nm) in THF ($1.5 \times 10^{-5}M$) at room temperature.

Decyloxy-substituted benzenedialdehyde **12** was synthesized according to procedures found in the literature.[28] Another monomer, diphosphonate **11** was synthesized in one step from the dibromide **10**, in almost quantitative yield. The Horner-Emmons reaction was also used to synthesize **PDOPV** under the same conditions as **PDDPV**. The formation of this polymer was confirmed by ^{1}H NMR and ^{13}C NMR, and by GPC.

Synthesis of the Alternating Copolymer, Poly(2,5-didecyl-1,4-phenylene vinylene-*alt*-2,5-didecyloxy-1,4-phenylene vinylene) (PDDPV-alt-DOPV). The synthetic strategy simply involved the same condensation procedure for the copolymer as the polymers, combining 2,5-didecylterephthalaldehyde **5** with 1,4-*bis*(-diethylphosphonate)-2,5-didecyloxybenzene **11** in anhydrous DMF making use of the Horner-Emmons reaction as shown in Scheme 3. The same precautions and processing methods used for preparing PDDPV were utilized in the preparation of the alternating copolymer. The formation of **PDDPV-alt-DOPV**, poly(2,5-didecyl-1,4-phenylene vinylene-*alt*−2,5-didecyloxy-1,4-phenylene vinylene), was confirmed by ^{1}H NMR, ^{13}C NMR, and GPC.

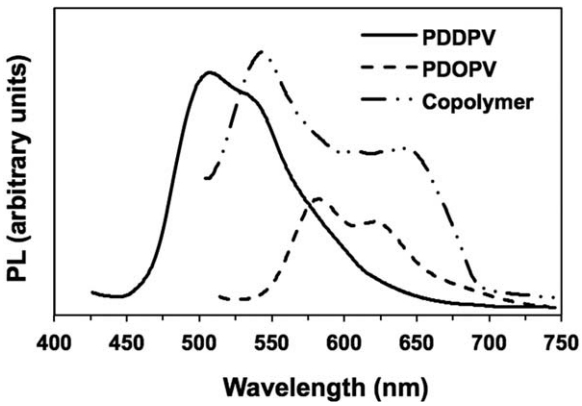

Figure 8. Film fluorescence spectra of **PDDPV** (excitation at 385 nm), **PDOPV** (excitation at 485 nm), and **PDDPV-alt-DOPV** (excitation at 470 nm) on quartz slides spin coated from solutions in ODCB (1 mg/mL).

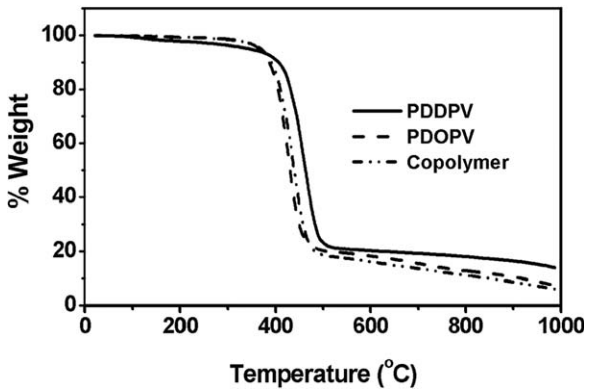

Figure 9. TGA thermograms of **PDDPV**, **PDOPV**, and **PDDPV-alt-DOPV**.

Molecular Weight Measurements. The data in Table I show the molecular weights of the polymers generated by the Horner-Emmons reaction. The low molecular weights are indicative of the poor solubility of the polymers. After multiple filtrations to attain processable solutions for the GPC, only the low molecular weight portions were analyzed by the instrument. The alternating copolymer had improved solubility so larger polymer chains could be detected. All samples had comparable polydispersities to those produced by the Gilch method in DMF.[31] Additional information regarding the molecular weight data can be found in the Supporting Information.

Absorption and Fluorescence Spectra. UV-Vis absorption and fluorescence spectra for the polymers were acquired with dilute solutions in THF under equivalent conditions for comparison. Figure 5 shows the UV-Vis absorption spectra of the three polymers prepared by the Horner-Emmons polymerization, **PDDPV**, **PDOPV**, and **PDDPV-alt-DOPV**. The major band in the spectra can be attributed to π-π^* transitions of the conjugated backbone.[32] The numerical values of the absorption maxima from THF solutions are given in Table I. It is worth noting that **PDOPV** exhibited a greater λ_{max} value than **PDDPV** (465 nm *vs.* 380 nm, respectively), suggesting a diminished conjugation length for the latter polymer. This blue shift, however, can be rationalized on the basis of the weaker electron-donating alkyl groups on the phenyl rings of **PDDPV** compared with the stronger electron-donating alkoxy groups for **PDOPV**; correspondingly, λ_{max} for **PDDPV-alt-DOPV** appears at 440 nm.[33] As expected, the absorption spectra in Figure 6 taken from thin films deposited on quartz slides are very similar to the solution-based measurements, with red shifts due to increased interchain interactions in the solid state.

Table II. Thermal Stability of the Polymers

Polymer	TGA T_d (°C)
PDDPV	425
PDOPV	394
PDDPV-alt-DOPV	406

TGA measurements were taken on samples with similar optical properties and higher molecular weights.

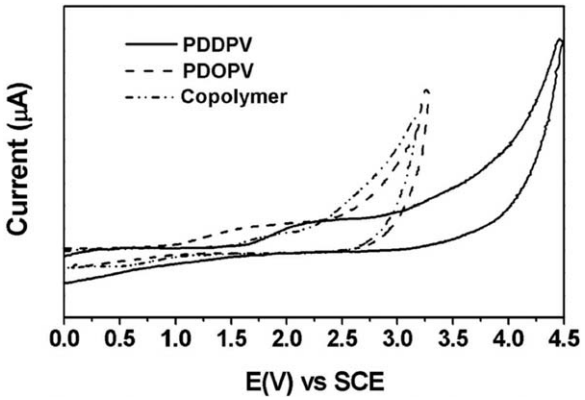

Figure 10. Cyclic voltammograms of **PDDPV**, **PDOPV**, and **PDDPV-alt-DOPV**, obtained under bubbling argon.

Figure 7 shows the fluorescence (FL) spectra of **PDDPV**, **PDOPV**, and **PDDPV-alt-DOPV** in THF obtained upon excitation at 380 nm, 465 nm, and 440 nm, respectively. The emission band of **PDDPV** appears at 496 nm while that of **PDOPV**, with its markedly stronger electron-donating groups, is substantially red-shifted to 535 nm. Reasonably, the emission band of **PDDPV-alt-DOPV** appears in between at 510 nm. All three polymers show discernable shoulder bands that are red-shifted by ~30 nm from their corresponding maxima, which is consistent with the vibronic coupling of excitons.[34] In Figure 8, a red shift is observed in the film-based FL spectra, which might be due to increased interchain interactions in the solid state.[35]

The quantum yield of each polymer was calculated relative to 9,10-diphenylanthracene and quinine sulfate because their emission spectra have the best spectral overlap to minimize variations in the detector response. Nevertheless, since the amount of overlap varies for each derivative, some variation could not be eliminated. The results given in Table I, and illustrated in Figure S15 in the Supporting Information, show that PDDPV has the highest quantum yield at ~57%. All the values are within the ranges found in literature for similar structures.[36–39]

Thermal Analysis. The thermal properties of samples with similar optical properties and higher molecular weights were evaluated by means of TGA by heating the samples at a rate of 10°C min^{-1} under an atmosphere of nitrogen. The data obtained are illustrated in Figure 9 and summarized in Table II. All three polymers possess good thermal stability, with decomposition temperatures (T_d, as defined by the extrapolated onset

Table III. Electrochemical Properties of PDDPV, PDOPV, and PDDPV-alt-DOPV in Solid Films in the Absence of O_2

Polymer	E_{ox} (V)	HOMO (eV)	UV Edge (nm)	EG (eV)	LUMO (eV)
PDDPV	1.75	−6.15	487	2.55	−3.60
PDOPV	1.20	−5.60	563	2.20	−3.40
PDDPV-alt-DOPV	1.50	−5.90	495	2.51	−3.39

CV measurements were taken on samples with similar optical properties and higher molecular weights.

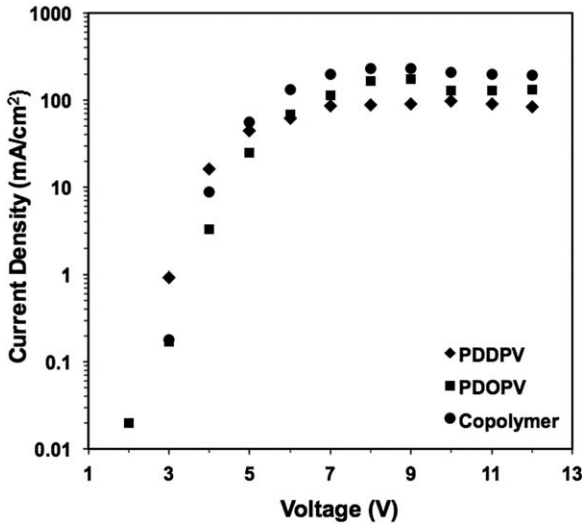

Figure 11. Current density-voltage characteristics of **PDDPV**, **PDOPV**, and **PDDPV-alt-DOPV** in ITO/PEDOT:PSS/Polymer/Alq3/LiF/Al devices.

of weight loss) ranging from 394°C to 425°C, with no significant weight loss at lower temperatures. The decomposition temperature of **PDDPV** is much higher than that of **PDOPV**, indicating that the alkyl chains enhance the thermal stability of this PPV-based polymer relative to that of the more common alkoxy-substituted derivatives. The enhanced thermal stability of the new PPV derivatives will perhaps lead to reduced rates of degradation of the EL emissive layer during the operation of the corresponding OLED devices.[34]

Electrochemical Properties. Cyclic voltammetry (CV) was employed to investigate the electrochemical behavior of samples with similar optical properties but higher molecular weight, as well as estimate the LUMO energy level of the materials. The oxidation process for such polymers is clearly discernible by CV and is directly associated with the conjugated structure of the

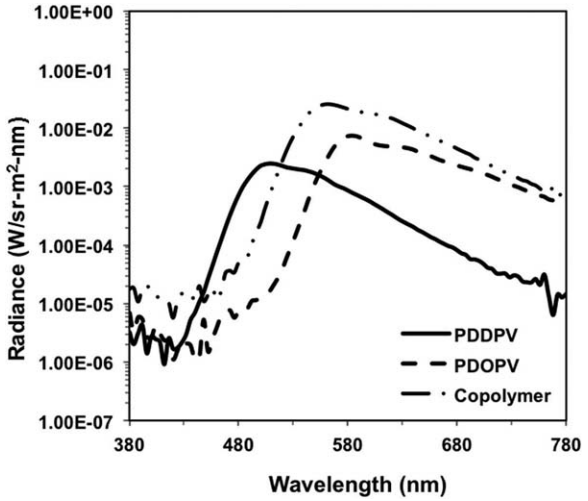

Figure 12. Electroluminescent spectrum of **PDDPV**, **PDOPV**, and **PDDPV-alt-DOPV** OLED devices fabricated with a configuration of ITO/PEDOT:PSS/Polymer/Alq3/LiF/Al.

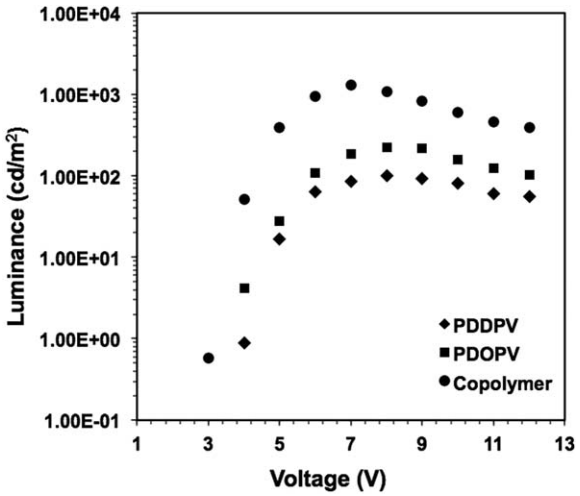

Figure 13. Luminance-voltage characteristics of **PDDPV**, **PDOPV**, and **PDDPV-alt-DOPV** in OLED devices fabricated with a configuration of ITO/PEDOT:PSS/Polymer/Alq3/LiF/Al.

polymer. However, the reduction process is usually irreversible and poorly defined. This behavior may be associated with polymer defects or traces of impurities.[40] For our analysis of the electrochemical properties of these polymers, films of the polymers were deposited on a Pt electrode and were analyzed only in the positive direction in a 0.10 M tetrabutylammonium hexafluorophosphate ($TBAPF_6$) solution of anhydrous acetonitrile. We structured our experiment in this manner because only onset potentials of the oxidation process were of interest and because one of the research objectives—that of improving device operation lifetime—is tied to such oxidative processes. Additionally, when the reduction potentials were analyzed, erratic behavior was observed due to irreversible oxidation. We utilized a system in which bubbling Ar into the solution of $TBAPF_6$ was intended to exclude atmospheric O_2.

Figure 10 shows cyclic voltammograms of all polymers during the oxidation process. The LUMO energy level of polymers can be calculated from the onset oxidation potential (E_{ox}(onset)) and the low energy absorption edge of the UV spectrum with the value in eV shown in eqs. (1) and (2).[32,41,42]

$$\text{HOMO (eV)} = -|E_{ox} + 4.4| \quad (1)$$

$$\text{LUMO(eV)} = \text{HOMO} - E_{\text{UV edge}}(\text{bandgap}) \quad (2)$$

In these equations, E_{ox} is the onset oxidation potential, and $E_{\text{UV edge}}$ is the absorption edge of the UV spectrum in units of electron volts (eV). The HOMO energy level of **PDDPV**, **PDOPV**, and **PDDPV-alt-DOPV** are −6.15 eV, −5.60 eV, and −5.90 eV, respectively. The low-energy edge of the UV-Vis absorption spectra (λ_{onset}) can be used to estimate the energy gap (EG) using eq. (3).[32]

$$\text{EG (eV)} = 1240/\lambda_{onset} \quad (3)$$

The energy gaps for our polymers range from 2.20 to 2.55 eV. The LUMO energy levels can be estimated using the HOMO from the electrochemical data and the bandgap from UV-Vis data. Table III summarizes the HOMO, LUMO, and EG values of **PDDPV**, **PDOPV**, and **PDDPV-alt-DOPV**. From Table III, we find that the HOMO and LUMO of **PDDPV** are much lower than those of the other two polymers. The energy gap of **PDOPV** is 2.20 eV, which is consistent with values for other dialkoxy derivatives obtained from the literature (i.e., 2.1 eV).[42]

One can observe from this system that the oxidation potential decreases with the attachment of alkoxy groups on the phenyl ring in the polymer chain. It is known that lowering the oxidation potential favors hole-injection, which provides an advantage for EL applications.[43] However, the oxidation potential of **PDDPV** is significantly higher than **PDOPV** and **PDDPV-alt-DOPV**. This can be explained with a conclusion that **PDOPV** is more readily oxidized as compared with **PDDPV**, implying a more stable emissive layer on OLEDs for the latter.

Device Studies. Light-emitting diode devices were fabricated in order to test the electroluminescent characteristics of the polymers, and to determine their viability for use in organic optoelectronic devices. On the basis of the band gap/energy level of the polymers, the ITO/PEDOT : PSS/polymer/Alq3/LiF/Al configuration was found suitable for our device architecture. Figure 11 compares the current density–voltage (*J–V*) characteristics of the devices. The current onsets are within an acceptable range of estimated band gap (0.5 eV).[44] **PDOPV** and **PDDPV-alt-DOPV** exhibited an EL turn-on voltage (defined as the voltage applied which produces 1 cd/m^2) at 4.0 V and **PDDPV** at 5.0 V.[45] Previous studies suggest that aggregation between conjugated polymer chromophores produces turn-on voltage differences.[46] Such aggregation, while advantageous for good carrier transport through the film, is also conducive to the formation of interchain excimers and polaron pairs, which reduce the luminescence efficiency.

The electroluminescent spectra are shown in Figure 12. The electroluminescent maxima are similar to the photoluminescent maxima (Figures 7 and 8). The alternating copolymer exhibited

Table IV. Electroluminescent Characteristics of OLEDs Containing PDDPV, PDOPV, and Their Alternating Copolymer

Polymer	Turn-on voltage[a] (eV)	EL brightness max (cd/m^2)	Max efficiency (cd/A)	λ_{maxEL} (nm) at 8 V)	1931 CIE Chromaticity (x, y) at 8 V
PDDPV	5.0	101.0	0.116	508, 76	0.31, 0.58
PDOPV	4.0	1300	0.725	560, 88	0.49, 0.51
PDDPV-alt-DOPV	4.0	223.0	0.164	584, 84	0.58, 0.42

Device configuration: ITO/PEDOT:PSS/Polymer/Alq3(30 nm)/LiF(8 nm)/Al(80 nm).
[a] With electroluminescence at 1 cd/m^2.

the highest radiance at 8.0 V, a result that might be attributable to solubility differences; **PDDPV** was the least soluble of the three polymers and produced thinner films. All three polymers reached a maximum luminance and began to dim as voltage was increased to 12 V (see Figure 13). This phenomenon might arise from increased charge leakage at the pixel edge where the Alq3 was thinnest. All devices exhibited an external quantum efficiency (EQE) of less than 1% due to the high current density (see Figure S16 in the Supporting Information). This measure of device performance can also be affected by charge leakage. A summary of the electroluminescent properties is given in Table IV, including CIE chromaticity coordinates.

Finally, one of the goals of this investigation centered on the use of the new polymeric components to enhance the active lifetimes of the devices, we have yet to establish definitively whether this objective has been met. We note, however, that a preliminary study using a more primitive device architecture suggests that the radiance of devices derived using PDDPV is more robust than that of devices derived from the other two polymers (see Supporting Information Figure S17). Future studies will explore this issue in greater detail.

CONCLUSIONS

Didecyl-substituted, didecyloxy-substituted, and didecyl-substituted alternating with didecyloxy-substituted PPV polymers, **PDDPV**, **PDOPV**, and **PDDPV-alt-DOPV**, respectively, were successfully synthesized by using an inexpensive and simple synthetic route, the Horner-Emmons polycondensation reaction. This approach afforded polymers with high molecular weights and low polydispersities. The presence of decyl and decyloxy side chains improves the solubility of the polymer and the ability to incorporate these polymers into devices. The associated ^{1}H NMR spectra exhibited peaks in the aromatic region corresponding to the aromatic and alkene protons, confirming the successful assembly of the conjugated polymer chain. UV-Vis absorption spectra and fluorescence spectra showed that **PDOPV** absorbed and emitted light at longer wavelengths than **PDDPV** and **PDDPV-alt-DOPV**. In addition, all three polymers exhibited good thermal stabilities, losing less than 10% of their weight on heating to approximately 400°C, which offers advantages under operational voltages. Organic-light emitting devices were fabricated from the synthesized polymers with a goal of achieving good emission of light under applied voltage. The study of these devices revealed that **PDDPV** possessed the highest turn-on electric field. We believe that our initial examination of the new PPV polymer structures indicate that they are promising candidates for LED applications.

ACKNOWLEDGMENTS

The authors thank the Robert A. Welch Foundation (Grant No. E-1320) and the Texas Center for Superconductivity at the University of Houston for generously supporting this research. The authors also acknowledge support from NSF PFI grant number IIP-1114211.

AUTHOR CONTRIBUTIONS

Crystal A. Young synthesized the monomers and polymers, characterized the materials, fabricated OLED devices, and wrote the manuscript. Dr. Sairoong Saowsupa contributed to the development of the synthetic procedures, produced an initial set of monomers and polymers, performed CV and TGA experiments, and wrote the manuscript. Audrey Hammack prepared the ITO slides and performed the cathode deposition. Dr. Andrew A. Tangonan contributed to the development of the synthetic procedures and assisted with the materials characterization. Dr. Piched Anuragudom contributed to the development of the synthetic procedures and assisted with the materials characterization. Dr. Huiping Jia assisted with OLED device fabrication and provided training on device measurements. Dr. Andrew C. Jamison contributed to the writing and editing of the manuscript. Dr. Sukon Panichphant contributed to the writing of the manuscript. Dr. Bruce E. Gnade supervised the device fabrication. Dr. T. Randall Lee conceived and supervised the research project; he also contributed to the writing and editing of the article.

REFERENCES

1. Yamamoto, T.; Usui, M.; Ootsuka, H.; Iijima, T.; Fukumoto, H.; Sakai, Y.; Aramaki, S.; Yamamoto, H. M.; Yagi, T.; Tajima, H.; Okada, T.; Fukuda, T.; Emoto, A.; Ushijima, H.; Hasegawa, M.; Ohtsu, H. *Macromol. Chem. Phys.* **2010**, *211*, 2138.
2. Vanormelingen, W.; Smeets, A.; Franz, E.; Asselberghs, I.; Clays, K.; Verbiest, T.; Koeckelberghs, G. *Macromolecules* **2009**, *42*, 4282.
3. Su, W.-F.; Chen, Y. *Polymer* **2011**, *52*, 77.
4. Xu, X.; Han, B.; Chen, J.; Peng, J.; Wu, H.; Cao, Y. *Macromolecules* **2011**, *44*, 4204.
5. Sandström, A.; Matyba, P.; Edman, L. *Appl. Phys. Lett.* **2010**, *96*, 053303.
6. Ding, T.; Zhao, B.; Shen, P.; Lu, J.; Li, H.; Tan, S. *J. Appl. Polym. Sci.* **2011**, *120*, 3387.
7. Qu, H.; Luo, J.; Zhang, X.; Chi. C. *J. Polym. Sci. Part A: Polym. Chem.* **2010**, *48*, 186.
8. Stathopoulos, N. A.; Palilis, L. C.; Vasilopoulou, M.; Botsialas, A.; Falaras, P.; Argitis, P. *Phys. Stat. Sol. A* **2008**, *205*, 2522.
9. Wang, H.; Li, F.; Ravia, I.; Gao, B.; Li, Y.; Medvedev, V.; Sun, H.; Tessler, N.; Ma, Y. *Adv. Funct. Mater.* **2011**, *21*, 3770.
10. Ha, Y.-G.; You, E.-A.; Kim, B.-J.; Choi, J.-H. *Synth. Met.* **2005**, *153*, 205.
11. Burroughes, J. H.; Bradley, D. D. C.; Brown, A. R.; Marks, R. N.; Mackay, K.; Friend, R. H.; Burns, P. L.; Holmes, A. B. *Nature* **1990**, *347*, 539.
12. Ervithayasuporn, V.; Abe, J.; Wang, X.; Matsushima, T.; Murata, H.; Kawakami, Y. *Tetrahedron* **2010**, *66*, 9348.
13. Stegmaier, K.; Fleissner, A.; Janning, H.; Yampolskii, S.; Melzer, C.; von Seggern, H. *J. Appl. Phys.* **2011**, *110*, 034507.
14. Mitschke, U.; Bäuerle, P. *J. Mater. Chem.* **2000**, *10*, 1471.
15. Geffroy, B.; le Roy, P.; Prat, C. *Polym. Int.* **2006**, *55*, 572.
16. Cumpston, B. H.; Jensen, K. F. *Synth. Met.* **1995**, *73*, 195.
17. Cumpston, B. H.; Parker, I. D.; Jensen, K. F. *J. Appl. Phys.* **1997**, *81*, 3716.

18. Scurlock, R. D.; Wang, B.; Ogilby, P. R.; Sheats, J. R.; Clough, R. L. *J. Am. Chem. Soc.* **1995**, *117*, 10194.
19. Ran, C.; Wang, M.; Gao, W.; Ding, J.; Shi, Y.; Song, X.; Chen, H.; Ren, Z. *J. Phys. Chem. C* **2012**, *116*, 23053.
20. Yan, H.; Lee, P.; Armstrong, N. R.; Graham, A.; Evmenenko, G. A.; Dutta, P.; Marks, T. J. *J. Am. Chem. Soc.* **2005**, *127*, 3172.
21. Hale, G. D.; Jackson, J. B.; Shmakova, O. A.; Lee, T. R.; Halas, N. J. *Appl. Phys. Lett.* **2001**, *78*, 1502.
22. Parekh, B. P.; Tangonan, A. A.; Newaz, S. S.; Sanduja, S. K.; Ashraf, A. Q.; Krishnamoorti, R.; Lee, T. R. *Macromolecules* **2004**, *37*, 8883.
23. Becker, H.; Spreitzer, H.; Kreuder, W.; Kluge, E.; Schenk, H.; Parker, I.; Cao, Y. *Adv. Mater.* **2000**, *12*, 42.
24. Jin, S.-H.; Park, H.-J.; Kim, J. Y.; Lee, K.; Lee, S.-P.; Moon, D.-K.; Lee, H.-J.; Gal, Y.-S. *Macromolecules* **2002**, *35*, 7532.
25. Anuragudom, P.; Newaz, S. S.; Phanichphant, S.; Lee, T. R. *Macromolecules* **2006**, *39*, 3494.
26. Aiamsen, P.; Anuragudom, P.; Saowsupa, S.; Phanichphant, S.; Lee, T. R. *J. Photopolym. Sci. Tech.* **2008**, *21*, 339.
27. Moy, C. L.; Kaliappan, R.; McNeil, A. J. *J. Org. Chem.* **2011**, *76*, 8501.
28. Shao, P.; Li, Z.; Luo, J.; Wang, H.; Qin, J. *Synth. Commun.* **2005**, *35*, 49.
29. Zhang, C.; Choi, S.; Haliburton, J.; Cleveland, T.; Li, R.; Sun, S.-S.; Ledbetter, A.; Bonner, C. E. *Macromolecules* **2006**, *39*, 4317.
30. Nomura, K.; Morimoto, H.; Imanishi, Y.; Ramhani, Z.; Geerts, Y. *J. Polym. Sci. Part A: Polym. Chem.* **2001**, *39*, 2463.
31. Parekh, B. P.; Tangonan, A. A.; Newaz, S. S.; Sanduja, S. K.; Ashraf, A. Q.; Krishnamoorti, R.; Lee, T. R. *Macromolecules* **2004**, *37*, 8883.
32. Chen, K.-B.; Li, H.-C.; Chen, C.-K.; Yang, S.-H.; Hsieh, B. R.; Hsu, C.-S. *Macromolecules* **2005**, *38*, 8617.
33. Cornil, J.; dos Santos, D. A.; Beljoune, D.; Bredas, J. L. *J. Phys. Chem.* **1995**, *99*, 5604.
34. Chen, Z.-K.; Lee, N. H. S.; Huang, W.; Xu, Y.-S.; Cao, Y. *Macromolecules* **2003**, *36*, 1009.
35. Nguyen, T.-Q.; Martini, I. B.; Liu, J.; Schwartz, B. J. *J. Phys. Chem. B* **2000**, *104*, 237.
36. Brouwer, H.-J.; Krasnikov, V. V.; Hilberer, A.; Wildeman J.; Hadziioannou, G. *Appl. Phys. Lett.* **1995**, *66*, 3404.
37. Kim, Y.; Swager, T. M. *Chem. Commun.* **2005**, 372.
38. Jakubiak, R.; Collison, C. J.; Wan, W. C.; Rothberg, L. J.; Hsieh, B. R. *J. Phys. Chem. A* **1999**, *103*, 2394.
39. Nguyen T.-Q.; Doan, V.; Schwartz B. J. *J. Chem. Phys.* **1999**, *110*, 4068.
40. Henckens, A.; Colladet, K.; Fourier, S.; Cleij, T. J.; Lutsen, L.; Gelan, J.; Vanderzande, D. *Macromolecules* **2005**, *38*, 19.
41. Bredas, J. L.; Silbey, R.; Boudreaux, D. S.; Chance, R. R. *J. Am. Chem. Soc.* **1983**, *105*, 6555.
42. Lee, Y.-Z.; Chen, X. W.; Chen, S.-A.; Wei, P.-K.; Fann, W.-S. *J. Am. Chem. Soc.* **2001**, *123*, 2296.
43. Yang, S.-H.; Chen, S.-Y.; Wu, Y.-C.; Hsu, C.-S. *J. Polym Sci. Part A: Polym. Chem.* **2007**, *45*, 3440.
44. Wang, X. J.; Zhao, J. M.; Zhou, Y. C.; Wang, X. Z.; Zhang, S. T.; Zhan, Y. Q.; Xu, Z.; Ding, H. J.; Zhong, G. Y.; Shi, H. Z.; Xiong, Z. H.; Liu, Y.; Wang, Z. J.; Obbard, E. G.; Ding, X. M.; Huang, W.; Hou, X. Y. *J. Appl. Phys.* **2004**, *95*, 3828.
45. Ye, H.; Chen, D.; Liu, M.; Su, S. -J.; Wang, Y. -F.; Lo, C. -C.; Lien, A.; Kido. J. *Adv. Funct. Mater.* **2014**, *24*, 3268.
46. Taranekar, P.; Abdulbaki, M.; Krishnamoorti, R.; Phanichphant, S.; Waenkaew, P.; Patton, D.; Fulghum, T.; Advincula, R. *Macromolecules* **2006**, *39*, 3848.